Gallbladder histopathology during murine gallstone formation: relation to motility and concentrating function

Karel J. van Erpecum,[1,2,*] David Q-H. Wang,[1,†] Antonio Moschetta,[§] Domenico Ferri,[**] Maria Svelto,[††] Piero Portincasa,[§§] Jan-Jaap Hendrickx,[***] Marguérite Schipper,[***] and Giuseppe Calamita,[††]

Department of Gastroenterology* and Department of Pathology,*** University Medical Center Utrecht, Utrecht, The Netherlands; Gastroenterology Division,† Beth Israel Deaconess Medical Center, Harvard Medical School, and Harvard Digestive Diseases Center, Boston, MA; Howard Hughes Medical Institute and Department of Pharmacology,§ University of Texas Southwestern Medical Center, Dallas, TX; and Department of Zoology, Laboratory of Histology and Comparative Anatomy,** Department of General and Environmental Physiology,†† and Section of Internal Medicine, Department of Internal and Public Medicine,§§ University of Bari, Bari, Italy

Abstract C57L mice are susceptible and AKR mice are resistant to gallstone formation. We studied in male mice of both strains gallbladder histopathology, cholecystokinin-induced emptying, and concentrating function at 0, 14, 28, and 56 days on a lithogenic diet. Gallbladder wall thickness increased on the diet, with stromal granulocyte infiltration, progressive fibrosis, edema, and epithelial cell indentation, particularly in C57L. Strong basal cholecystokinin octapeptide-induced gallbladder emptying (70% of fasting volumes) occurred in both strains, but fasting gallbladder volumes were significantly larger in C57L (14.8 ± 2.2 μl vs. 8.8 ± 1.0 μl). On the diet, fasting volumes increased exclusively in C57L (28.6 ± 2.9 μl on day 56), with progressively decreased emptying (27% of fasting volumes on day 56). Gallbladder emptying remained normal in AKR. Gallbladder concentrating function decreased on the lithogenic diet (especially in C57L), coinciding with decreased aquaporin-1 (AQP1) and AQP8 expression at the mRNA and protein levels. In additional experiments, similar downregulation of AQP1 and AQP8 mRNA expression occurred in farnesoid X receptor (FXR)-deficient mice after 1 week on the lithogenic diet, without any difference from corresponding wild-type mice. In conclusion, during murine lithogenesis, altered gallbladder histology is associated with impaired motility, reduced concentrating function, and decreased AQP1 and AQP8 expression, the latter without the involvement of the FXR.—van Erpecum, K. J., D. Q-H. Wang, A. Moschetta, D. Ferri, M. Svelto, P. Portincasa, J-J. Hendrickx, M. Schipper, and G. Calamita. **Gallbladder histopathology during murine gallstone formation: relation to motility and concentrating function. *J. Lipid Res.* 2006.** 47: **32–41.**

Supplementary key words aquaporin • cholesterol • farnesoid X receptor • gallbladder emptying • water channel

C57L and AKR inbred mice exhibit different susceptibilities to cholesterol gallstone formation, depending on *Lith* genes. Susceptibility is high in C57L males (gallstones in 80% of mice after 56 days on a lithogenic diet) and low in AKR males (gallstones in 15% after 56 days on a lithogenic diet) (1). Based on their time course during the earliest stages of lithogenesis, biliary cholesterol supersaturation, the hydrophobic bile salt deoxycholate, and high concentrations of crystallization-promoting mucin are thought to play crucial roles in murine gallstone formation (1, 2). In humans, the gallbladder is thought to be another key player in gallstone pathogenesis. Impaired postprandial and interdigestive gallbladder emptying are often found in gallstone patients, providing time for nucleation of cholesterol crystals and their aggregation into macroscopic stones (3). Also in animal models, gallbladder contractility is decreased in the earliest stages of gallstone formation, even before gallstones have formed (4). Furthermore, in the fasting gallbladder, hepatic bile is concentrated 4- to 5-fold by absorption of water, thereby enhancing cholesterol crystallization (5, 6). Aquaporins (AQP0 to AQP10) are a family of transmembrane channels mediating the movement of water through the lipid bilayer. AQP1 (7–12) and AQP8 (12) have recently been detected in gallbladder epithelial cells. Virtually no information is available about the gallbladder in murine gallstone formation, despite the obviously crucial role of this organ in lithogenesis.

In the present study, we describe gallbladder histopathology (including reduced AQP expression), motility, and

Manuscript received 9 May 2005 and in revised form 6 October 2005.

Published, JLR Papers in Press, October 13, 2005.
DOI 10.1194/jlr.M500180-JLR200

Abbreviations: CCK, cholecystokinin octapeptide; FXR, farnesoid X receptor.

[1] K. J. van Erpecum and D. Q-H. Wang contributed equally to this work.

[2] To whom correspondence should be addressed.
e-mail: k.j.vanerpecum@azu.nl

concentrating function on a lithogenic diet. Farnesoid X receptor (FXR: NR1H4) functions as a bile salt receptor regulating the transcription of numerous genes involved in cholesterol and bile salt homeostasis (13). This nuclear receptor may be relevant for gallstone formation: FXR-deficient ($FXR^{-/-}$) mice were recently found to exhibit high susceptibility to cholesterol gallstone formation (14). In addition, in gallstone-susceptible C57L mice on a lithogenic diet, biliary cholesterol supersaturation and gallstone formation were prevented by treatment with a synthetic FXR agonist: FXR-dependent increases in biliary secretion of cholesterol-solubilizing bile salt and phosphatidylcholine molecules restored cholesterol solubility and thereby prevented gallstone formation (14). Because the lithogenic diet contains cholic acid [a high-affinity ligand for FXR (15)], we investigated in the $FXR^{-/-}$ murine model whether the FXR pathway could play a direct role in reducing AQP gene expression.

MATERIALS AND METHODS

Animals

Homozygous male C57L/J and AKR/J mice were obtained from the Jackson Laboratory (Bar Harbor, ME). They were housed in a temperature-controlled room (22 ± 1°C) with a 12 h light cycle (6 AM–6 PM), with free access to water and Purina laboratory chow containing traces (<0.02%) of cholesterol (Harlan Teklad Laboratory Animal Diets, Madison WI). Once animals achieved 8 weeks of age, they were fed a semisynthetic lithogenic diet containing (per 100 g) 15 g of dairy fat, 1 g of cholesterol, 0.5 g of cholic acid, 2 g of corn oil, 50 g of sucrose, 20 g of casein, and essential vitamins and minerals (16). Cholecystectomy was performed and gallbladder bile was aspirated completely at 9 AM before (day 0) and after feeding the lithogenic diet for 14, 28, and 56 days (five mice of each strain at each time point). Gallbladders were immediately placed in formalin. Cholecystectomy and gallbladder bile collection were followed by cannulation of the common bile duct and hepatic bile collection for 1 h (1, 17, 18). Pooled gallbladder biles and individual hepatic biles (five mice at each time point) were stored at −20°C until further analysis. In a second and a third series of experiments, the effects of a lithogenic diet on AQP1 and AQP8 mRNA expression and on gallbladder motility were examined (five mice of each strain at each time point in all experimental groups). Gallbladder emptying was determined in fasted mice by intravenous injection of sulfated cholecystokinin octapeptide (CCK-8; 17 nmol/kg body weight dissolved in 100 μl of PBS), identical volumes of PBS, or no injection. Exactly 15 min after the injection, cholecystectomy was performed and gallbladder volume was determined (19, 20). A fourth series of experiments was performed in male $FXR^{-/-}$ mice (21). $FXR^{-/-}$ and wild-type mice were on the same mixed background (C57BL/6N×129/SVJ×FVB, backcross ×C57BL/6N). Experimental conditions were the same as described above. Mice were maintained on a low-cholesterol (0.02%) Purina chow diet until 9 weeks of age, followed by only 1 week of the lithogenic diet, given the sensitivity of $FXR^{-/-}$ mice to cholic acid (21). After 12 h of fasting, cholecystectomies were performed, and gallbladders were frozen in liquid nitrogen and stored at −80°C until further analysis. Protocols were approved by the Institutional Animal Care and Use Committee of Harvard University and by the Institutional Animal Care and Research Advisory Committee of the Southwestern Medical Center at Dallas and were consistent with euthanasia recommendations of the American Veterinary Medical Association.

Lipid analyses

Bile samples were lipid-extracted (22) after a short centrifugation (5 min at 3,000 *g*) to spin down cholesterol crystals. Cholesterol (23) and phospholipid (24) concentrations were measured enzymatically in the extracted biles, and total bile salt concentrations in whole biles were measured by the 3α-hydroxysteroid dehydrogenase method (25). The cholesterol saturation index was calculated according to the critical tables (26). Gallbladder bile samples were examined for the presence of cholesterol crystals using direct and polarizing light microscopy (100× and 400× magnification). Conjugated bile salt species were analyzed by HPLC (27) using a C-18 Waters Bondapack 10 μm column. Methanol-phosphate buffer was used as an eluent (pH 5.2, flow rate of 1 ml/min).

Histology

Histological evaluations were performed by two independent pathologists unaware of mouse strains or time on the lithogenic diet (5 μm sections from paraffin-embedded tissue), with high interobserver agreement. For each gallbladder, numbers of granulocytes were scored after hematoxylin-eosin staining in 20–40 high-power fields (400× magnification). For each gallbladder, wall thickness is the mean value of six determinations in the fundic area. Relative amounts of smooth muscle cells compared with relative amounts of fibrosis were scored in Azan-stained sections.

Immunohistochemistry and Western blots

Endogenous peroxidase was preliminarily blocked and gallbladder sections were then incubated overnight at 4°C with purified monospecific primary antibodies directed against the C terminus of AQP1 or AQP8 (anti-AQP1 or anti-AQP8; Alpha Diagnostic International) at a final concentration of 5 μg/ml in blocking buffer (1% normal goat serum in phosphate-buffered saline) (28). Thereafter, sections were washed and incubated with

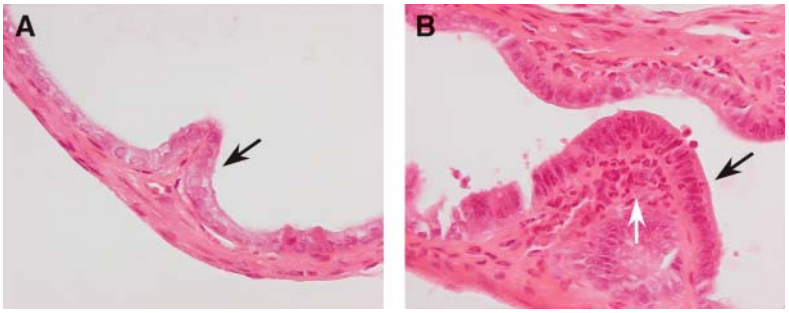

Fig. 1. Gallbladder histology of resistant AKR (A) and susceptible C57L (B) mice at baseline (hematoxylin-eosin; 400× magnification). Black arrows indicate the epithelial layer, and the white arrow indicates granulocyte infiltrate in C57L.

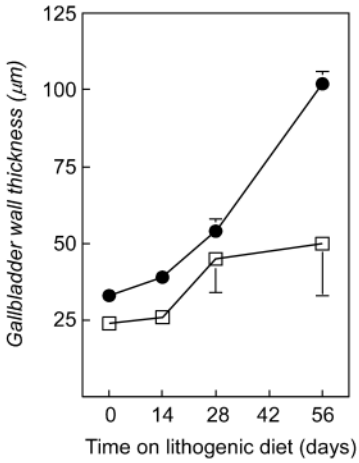

Fig. 2. Gallbladder wall thickness as a function of time on the lithogenic diet. Gallbladder wall thickness increases progressively during the diet period ($P < 0.0001$) and is more pronounced in C57L than in AKR ($P < 0.02$). Closed circles, C57L; open squares, AKR. Results are shown as means ± SEM.

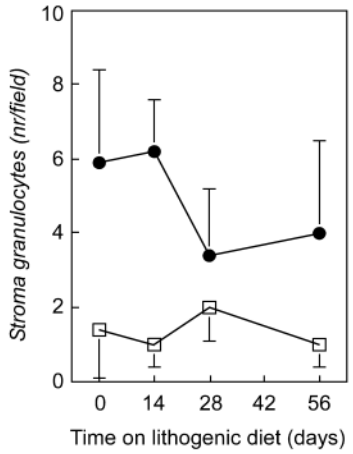

Fig. 3. Gallbladder stromal granulocytes (number/high-power field; 400× magnification) as a function of time on the lithogenic diet. Numbers of stromal granulocytes are significantly higher in C57L than in AKR ($P < 0.003$), but there are no changes during the diet period. Closed circles, C57L; open squares, AKR. Results are shown as means ± SEM.

goat anti-rabbit IgG (Sigma, St. Louis, MO). After several washes, the sections were incubated with horseradish peroxidase-antiperoxidase, and immunolabeling was visualized by incubation with 3,3′-diaminobenzidine-H_2O_2 (29). Controls performed using antibodies preadsorbed with immunizing peptides or by omitting the primary antibodies were always negative. Images were captured using a Nikon E600 photomicroscope equipped with a digital camera (Nikon DMX1200; Nikon Instruments S.p.a., Sesto Fiorentino, Italy). The intensity of AQP staining was scored with the aid of a semiquantitative score (0 = absent; 1+ = minor; 2+ = moderate; 3+ = appreciable; 4+ = strong) by one investigator (M. Svelto) unaware of mouse strain or time on the lithogenic diet. To quantitate gallbladder protein concentrations of AQP1 and AQP8, Western blot analysis was performed in separate sets of mice from both strains (n = 35 per group) before and after 28 and 56 days of feeding the lithogenic diet with the aid of anti-AQP1 or anti-AQP8 (Alpha Diagnostic Int.) and β-actin as a control.

Quantitative real-time PCR assays of *Aqp1* and *Aqp8* genes

Total RNA was extracted from C57L and AKR gallbladders using RNeasy Midi (Qiagen, Valencia, CA). Reverse-transcription reaction was performed using the SuperScript II First-Strand Synthesis System (Invitrogen, Carlsbad, CA) with 5 μg of total RNA and random hexamers to generate cDNA. Primer Express Software (Applied Biosystems, Foster City, CA) was used to design the following primers: mouse *Aqp1* (NM_007472) forward (5′-TTCCCCTTTGGTCTGACTTACC-3′), reverse (5′-TCAGCACAGGGACAATTCCA-3′), and probe (5′-AGGACCCTT-CCCCTTGAACTCACTCTAAGACC-3′); mouse *Aqp8* (NM_007474) forward (5′-CAGTCTGTGACCTAGAGATAAGTGAGTACA-3′), reverse (5′-GATCCGAGCCAGAGCTACCA-3′), and probe (5′-AGGGCAGCCGGCGAACGTC-3′). Real-time PCR assays for all samples were performed in triplicate on the GeneAmp 5700 Sequence Detection System (Applied Biosystems). Relative mRNA levels were calculated using the threshold cycle of an unknown sample against a standard curve with known copy numbers. Data were normalized using endogenous GAPDH as the invariant control (part 4308313; Applied Biosystems). For $FXR^{-/-}$ mice, RNA extraction from gallbladder was performed using the RNA STAT-60 reagent (Tel-Test B, Inc., Friendswood, TX). RNA was treated with RNase-free DNase (Roche, Diagnostics Corp., Indianapolis, IN) and reverse-transcribed (SuperScript II; Invitrogen) using random hexamers (Roche) to a final concentration of 20 ng/μl. Primer sequences were as follows: AQP1 forward (5′-CCTGCT-GGCGATTGACTACA-3′) and reverse (5′-GCACAGCAGAGCCAAAT-GAC-3′); AQP8 forward (5′-GTAGCTCTGGCTCGGATCTTC-3′) and reverse (5′-CCTTGACCTCAGGTAGGTCCAT-3′). Real-time quantitative PCR was performed as described previously (30) using SYBR Green I chemistry (SYBR Green PCR Master Mix; ABI)

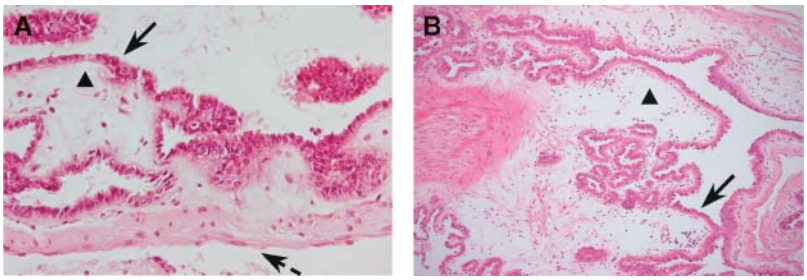

Fig. 4. A: Subepithelial edema in AKR mice at the end of the study period (56 days). B: More pronounced subepithelial edema in C57L mice after 56 days on the lithogenic diet, with significant granulocyte infiltrate. Arrows indicate the epithelial layer, the interrupted arrow indicates the smooth muscular layer, and the arrowhead indicates subepithelial edema (hematoxylin-eosin; 200× magnification).

on the ABI Prism 7900HT Sequence Detection System. Each sample was run in triplicate. Relative fold changes were calculated using the comparative cycle times method with cyclophilin as the reference gene and the wild-type mice as the calibrators.

Statistical analysis

Results are shown as means ± SEM. Differences between groups and time effects were analyzed for statistical significance by Mann-Whitney *U*-tests or ANOVA with Fisher's least significant difference as the posthoc test. A two-tailed *P* value of <0.05 was considered significant.

RESULTS

Gallbladder histology

At baseline, gallbladder wall thickness was greater, and epithelial cells appeared more elongated, in C57L than in AKR (**Figs. 1, 2**). On the lithogenic diet, gallbladder wall thickness increased markedly, but this was most pronounced in C57L (Fig. 2). Also, there was moderate infiltration of neutrophilic granulocytes in gallbladder wall stroma and some intraepithelial granulocytes in C57L during the entire study period (Figs. 1B, **3**). Granulocytes were infrequent in AKR (Fig. 1A, 3), but occasional lymphoid aggregates were noted during the diet period. From day 28 on, progressive fibrosis (C57L > AKR) and, more pronounced, increased smooth muscle thickness were noted in the gallbladder wall. Also from day 28, sporadic macrophages loaded with debris and fat were seen in C57L. These abnormalities were progressive on day 56 in C57L, with concomitant edema in the subepithelial layer (**Fig. 4B**). Similar changes were not noted before day 56 in AKR and were less pronounced than for C57L (Fig. 4A). Also, progressive epithelial indentation was seen in C57L from day 28 of lithogenic feeding (**Figs. 5F, H, 6F, H**).

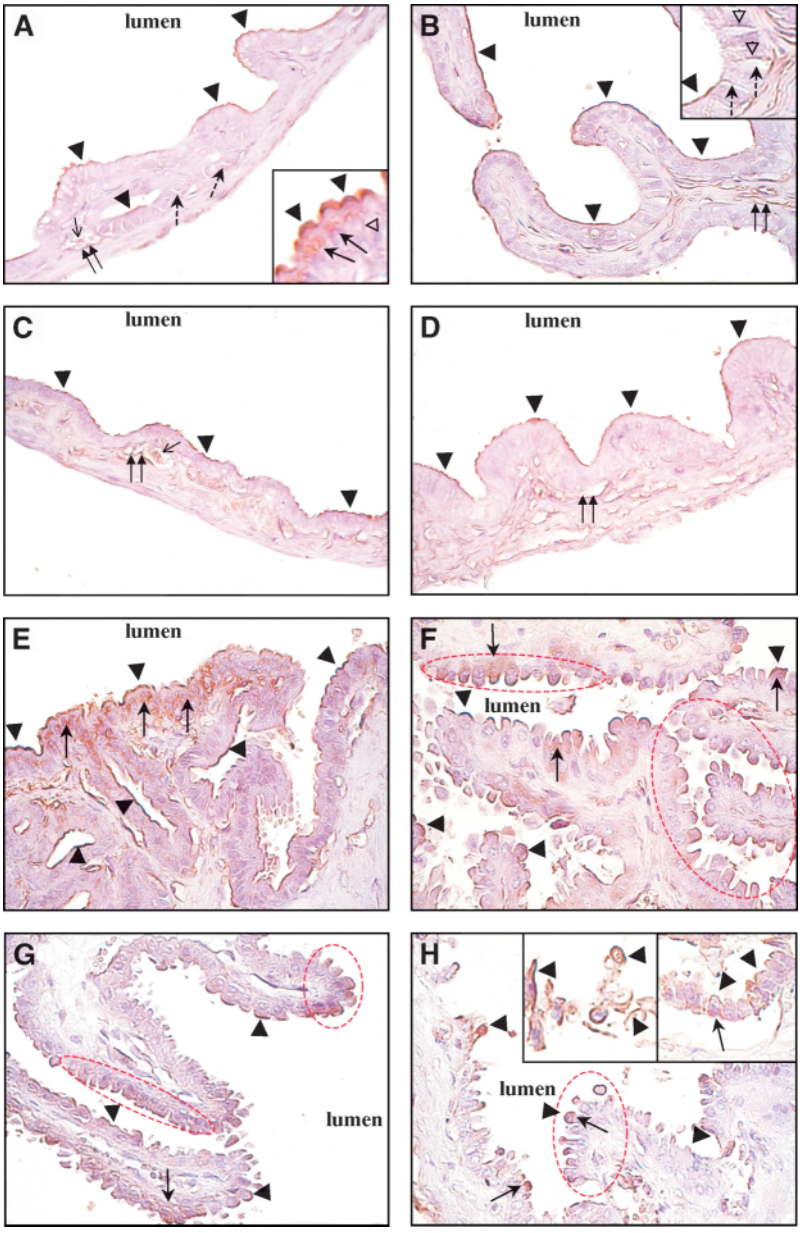

Fig. 5. Immunohistochemical distribution of aquaporin-1 (AQP1) in the gallbladders of AKR (A, C, E, G) and C57L (B, D, F, H) mice on the lithogenic diet. A, B: Day 0. Considerable AQP1 immunoreactivity (brown staining) is observed over the apical (arrowheads) and lateral (insets; open arrowheads) membranes of AKR (A) and C57L (B) gallbladder epithelia. Staining is also observed over the plasma membrane of endothelial cells (A,B; double arrows) and red blood cells (A; thin arrow). Additional labeling is often present in the neck region of both AKR and C57L gallbladders, where intracellular staining is seen over vesicles located at the subapical pole of surface epithelial cells (A, inset; arrows). Lateral spaces between adjacent epithelial cells appear enlarged as a morphological consequence of the process of fluid absorption (48) (B, inset; dashed arrows). C, D: Day 14. Immunohistochemical patterns of AQP1 in AKR (C) and C57L (D) gallbladder epithelial cells and plasma membranes of endothelial or red blood cells (apical staining, arrowheads; endothelial staining, double arrows; red blood cell staining, small arrows). E, F: Day 28. Considerable AQP1 expression (arrowheads) is seen at the apical pole of the gallbladder epithelium of both AKR (E) and C57L (F) mice. Subapical staining is frequently observed in the neck region of gallbladders (arrows). A striking indentation of the surface epithelial layer (red dashed areas) is observed in the C57L gallbladders (F). G, H: Day 56. Apical (arrowheads) and subapical (arrows) AQP1 labeling is present in the epithelial layer of both AKR (G) and C57L (H) gallbladders. Indentation of the epithelium is now also observed in the neck region of the AKR gallbladder (G; red dashed areas). AQP1 immunoreactivity is observed even in epithelial sheets detached away from the C57L gallbladder as a consequence of advanced lithogenesis (H, inset). Original magnifications, ×400.

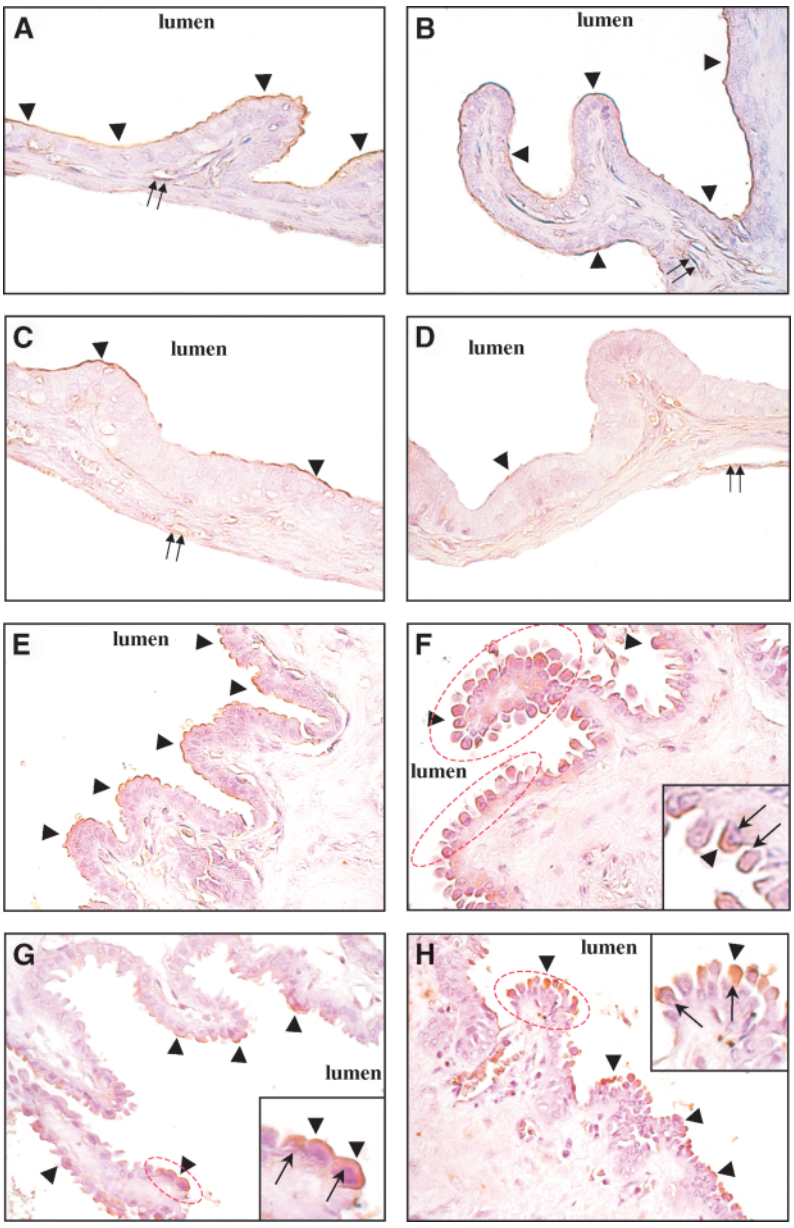

Fig. 6. Immunohistochemical expression of AQP8 in AKR and C57L gallbladders during lithogenic diet feeding. A, B: Day 0. Considerable AQP8 immunoreactivity (arrowheads) is seen at the apical pole of both AKR (A) and C57L (B) gallbladder. Some staining is also observed over the plasma membrane of endothelial cells (double arrows). C, D: Day 14. Although much less pronounced than on day 0, AQP8 reactivity is observed at the apical pole of both AKR (C) and C57L (D) gallbladders (arrowheads). The decrease in apical AQP8 expression is more pronounced in C57L (D; arrowheads) than in AKR gallbladders. Expression of AQP8 in both AKR and C57L gallbladder endothelial cells (double arrows) appears unchanged compared with basal values. E, F: Day 28. Apical labeling of AQP8 in AKR gallbladder epithelium (E; arrowheads) and C57L gallbladder epithelium (F; arrowheads). Note the intracellular reactivity (F, inset; arrows) often associated with the characteristic indentation of the C57L gallbladder epithelium (F; red dashed areas). G, H: Day 56. Considerable AQP8 reactivity is seen at the apical pole of both AKR (G) and C57L (H) gallbladders (arrowheads). Subapical reactivity (insets; arrows) is seen below the indentation (red dashed areas). Original magnifications, ×400.

Although less marked than in C57L, indented epithelium was also observed in AKR gallbladders at day 56 on the lithogenic diet (Figs. 5G, 6G).

Gallbladder motility

Basal fasting gallbladder volumes were significantly larger in C57L than in AKR inbred mice (14.8 ± 2.2 μl vs. 8.8 ± 1.0 μl). PBS infusion did not affect gallbladder volumes before or during diet treatment (**Fig. 7**). Before the lithogenic diet, low gallbladder volumes were observed after CCK infusion in both strains (4.4 ± 0.5 μl and 3.0 ± 0.3 μl in C57L and AKR, respectively, corresponding to 70% emptying). As shown in Fig. 7B, fasting gallbladder volumes increased progressively on the diet in C57L (from 14.8 ± 2.2 μl on day 0 to 28.6 ± 2.9 μl on day 56), with progressively decreased CCK-induced emptying (70% and 27% of fasting volumes on day 0 and day 56, respectively). In contrast, there were only minor (nonsignificant) increases of fasting gallbladder volumes in AKR during the lithogenic diet feeding (from 8.8 ± 1.0 μl on day 0 to 13 ± 1.3 μl on day 56), and CCK-induced gallbladder emptying remained largely preserved (Fig. 7A).

Biliary lipids and gallbladder concentrating function

The cholesterol saturation index in hepatic biles (basal, 0.91 ± 0.12 and 0.83 ± 0.12 for C57L and AKR, respectively) and associated gallbladder biles (basal, 0.53 and 0.52 for C57L and AKR, respectively) was supersaturated from day 14 in both strains. At baseline, mol% bile salts, cholesterol, and phospholipids in gallbladder biles and associated hepatic biles were identical. In contrast, during lithogenic diet feeding, mol% bile salts was consistently

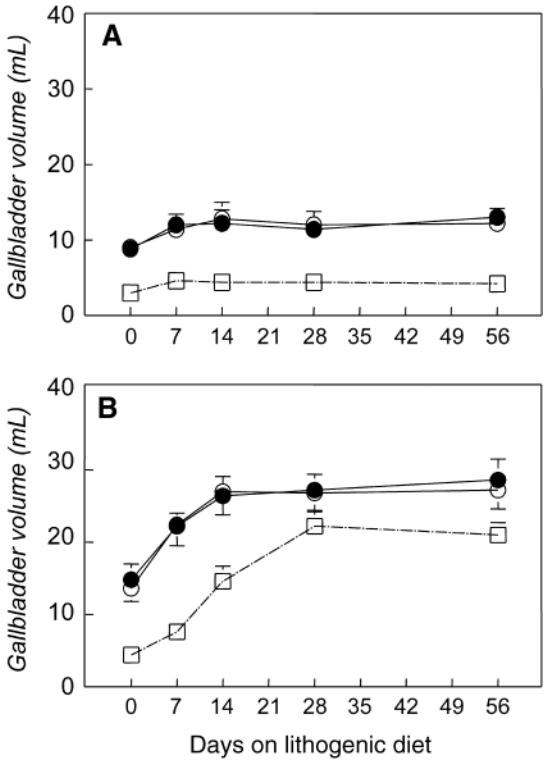

Fig. 7. Gallbladder motility in AKR (A) and C57L (B) mice as a function of time on the lithogenic diet. In C57L, there are highly significant increases of fasting gallbladder volumes (day 0 significantly different from all other time points) and highly significant decreases of cholecystokinin octapeptide (CCK)-induced gallbladder emptying (day 0 significantly different from all other time points) on the lithogenic diet. In contrast, there are only minor (nonsignificant) changes of fasting gallbladder volumes and preserved gallbladder emptying in AKR mice. Closed circles, control group; open circles, PBS infusion group; open squares, CCK infusion group. Results are shown as means ± SEM.

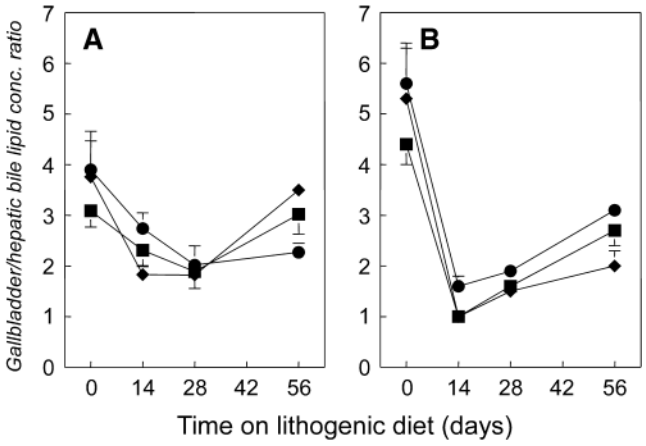

Fig. 8. Gallbladder-to-hepatic bile ratios of bile salt, phospholipid, and cholesterol concentrations in AKR (A) and C57L (B) mice before and during the lithogenic diet period. There are marked decreases in these ratios during lithogenic diet feeding, consistent with the loss of gallbladder absorptive function, particularly in C57L mice. Closed circles, ratio for bile salts; closed squares, ratio for cholesterol; closed diamonds, ratio for phospholipid. Results are shown as means ± SEM.

higher and mol% cholesterol and phospholipids were consistently lower in gallbladder biles than in associated hepatic biles (results not shown). During lithogenic diet feeding, the bile salt pool (at baseline mainly tauro-β-muricholate and taurocholate) became enriched in hydrophobic bile salts in C57L (taurochenodeoxycholate to 25± 2% and taurodeoxycholate to 9 ± 1%) but remained low in AKR. Cholesterol crystals were abundant from day 14 on in C57L, whereas only occasional crystals occurred in AKR at the end of the study period. Furthermore, as shown in **Fig. 8A, B**, the ratios of gallbladder bile to hepatic bile lipid concentration (at baseline, ~4 in AKR and ~5 in C57L) decreased markedly on the lithogenic diet, most pronounced in C57L mice (ratios at day 14, ~2.5 in AKR and ~1.5 in C57L). Decreases in these ratios are consistent with decreased gallbladder absorptive function during the lithogenic diet period.

AQP expression

Under basal conditions, AQP1 labeling was observed in both strains over the apical plasma membrane of the entire gallbladder epithelium (Fig. 5A, B). There was also some basolateral staining (Fig. 5B, inset). Immunoreactivity was most pronounced in the gallbladder neck region, where additional staining was frequently observed in intracytoplasmic vesicles at the subapical pole (Fig. 5A, inset). AQP1 immunolabeling was also observed over the plasma membrane of red blood cells and endothelial cells (Fig. 5A, thin arrow and double arrows, respectively). Overall, the immunohistochemical pattern in AKR (Fig. 5A, C, E, G) was similar to that of the corresponding C57L gallbladders (Fig. 5B, D, F, H). AQP1 reactivity remained detectable in indented epithelial cells at the end of the study period (Fig. 5H). On a semiquantitative scale (see Materials and Methods), AQP1 immunoreactivity decreased significantly in C57L from 3.8 ± 0.4 at baseline to 2.6 ± 0.5 at day 14 and in AKR from 3.8 ± 0.4 at baseline to 2.8 ± 0.4 at day 14.

Under basal circumstances, AQP8 immunoreactivity was detected mainly in the apical plasma membrane of the gallbladder epithelium of both AKR and C57L mice (Fig. 6A, B). Indented gallbladder epithelium at the end of the study period was often associated with the presence of AQP8 immunoreactivity at the subapical pole of the epithelial cell (Fig. 6G, H). In C57L and, less pronounced, AKR inbred mice, gallbladder epithelial expression of AQP8 was considerably reduced on the lithogenic diet (especially in the corpus-fundus region) compared with basal values (Fig. 6). On a semiquantitative scale (see Materials and Methods), AQP8 immunoreactivity decreased significantly in C57L from 3.8 ± 0.4 at baseline to 1.8 ± 0.4 at day 14 and in AKR from 3.6 ± 0.5 at baseline to 2.6 ± 0.5 at day 14. In agreement with the immunohistochemistry results, Western blots revealed significantly decreased AQP1 and AQP8 protein on the lithogenic diet in both strains (**Fig. 9**). By Western blot, AQP1 and AQP8 protein

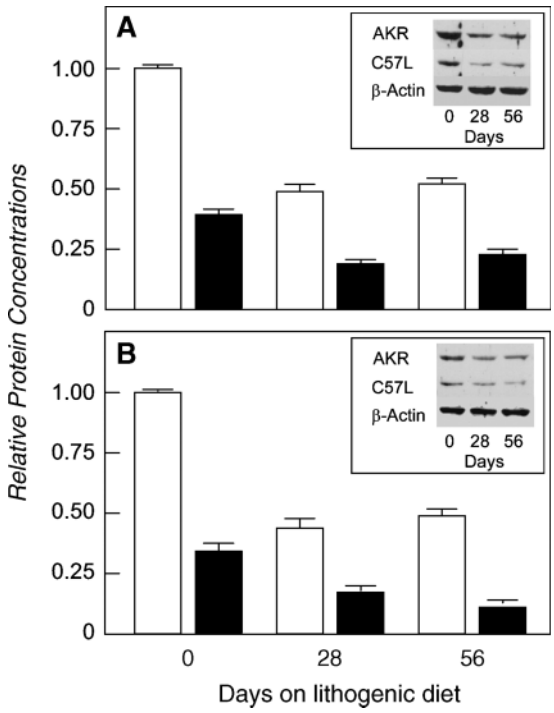

Fig. 9. Protein concentrations of AQP1 (A) and AQP8 (B) in gallbladders of mice (n = 35 per group) before and during lithogenic diet feeding for 56 days. For each protein concentration, the fold change for AKR mice (open bars) fed the lithogenic diet and C57L mice (closed bars) on chow or fed the lithogenic diet is expressed relative to chow-fed AKR mice, which is arbitrarily set at 1.0. Values represent means ± SEM of the fold change found in these mice.

levels were lower in C57L than in AKR. Relative AQP1 and AQP8 mRNA expression also decreased significantly in both strains after institution of the lithogenic diet (**Table 1**).

At baseline, gene expression of AQP1 and AQP8 in gallbladders of mice lacking the bile salt nuclear receptor FXR and corresponding wild-type mice did not differ. After 1 week of lithogenic diet feeding, significant decreases of gallbladder gene expression for AQP1 (±50% of the basal value) and AQP8 (±60% of the basal value) occurred in both $FXR^{-/-}$ and wild-type mice. Finally, no changes in AQP1 and AQP8 gene expression occur in wild-type mice treated with a synthetic FXR agonist (A. Moschetta and D. J. Mangelsdorf, unpublished observations).

DISCUSSION

Virtually no information is available about the gallbladder in the mouse model of gallstone formation, despite the obviously crucial role of this organ in murine lithogenesis. Therefore, we studied in detail gallbladder histopathology and function on a lithogenic diet in gallstone-susceptible C57L and gallstone-resistant AKR inbred mice. The results can be summarized as follows: *1*) progressive

TABLE 1. Relative AQP1 and AQP8 mRNA expression (corrected for GAPDH) decreases significantly in C57L and AKR inbred mice on the lithogenic diet

	AQP1		AQP8	
Time on the Lithogenic Diet	AKR	C57L	AKR	C57L
0 days	7.1 ± 0.4[a]	5.3 ± 0.2[a]	7.6 ± 0.3[a]	5.6 ± 0.2[a]
14 days	3.7 ± 0.2	2.8 ± 0.1	6.0 ± 0.2	3.1 ± 0.07
28 days	3.8 ± 0.2	2.7 ± 0.2	4.1 ± 0.2	2.9 ± 0.04
56 days	4.9 ± 0.2[a]	3.3 ± 0.2	5.0 ± 0.1	3.4 ± 0.1

AQP, aquaporin.
[a] Significantly different from all other time points.

changes in histology, most pronounced in C57L mice; *2*) progressive impairment of gallbladder emptying, exclusively in C57L; and *3*) impaired gallbladder concentrating function, most pronounced in C57L, coinciding with impaired expression at the mRNA and protein levels of the water channels AQP1 and AQP8.

Although there was moderate infiltration of granulocytes in C57L, this did not increase during the study period. Apparently, acute cholecystitis does not occur in the mouse model. Instead, fasting gallbladder volumes increased progressively in C57L, with progressive impairment of CCK-induced gallbladder emptying, very similar to human cholesterol gallstone patients (3). Changes in gallbladder motility may theoretically result from lithogenic gallbladder bile. In in vitro studies, significant amounts of cholesterol are absorbed by the gallbladder wall from supersaturated bile (31), with subsequent incorporation of the sterol within the sarcolemnal plasma membrane of the smooth muscle cell, leading to impaired motility (32). In the present study, basal mol% lipids in hepatic and gallbladder biles did not differ. In contrast, on the lithogenic diet, mol% bile salts were always higher and mol% cholesterol and phospholipids were always lower in gallbladder than in associated hepatic biles. These changes in the relative lipid composition of gallbladder compared with hepatic bile have also been reported in human gallstone patients (33, 34) and are consistent with cholesterol, and phospholipid, absorption (possibly from vesicular phases) by the gallbladder wall in the case of supersaturated bile. Indeed, candidate transport proteins for cholesterol, such as ABCG5/G8 (35), scavenger receptor class B type I (36), and megalin (37), have been detected in the human gallbladder wall. Alternatively, hydrophobic bile salts such as deoxycholate may impair gallbladder motility (38). Indeed, in the current study, hydrophobic bile salts (taurodeoxycholate and taurochenodeoxycholate) were found in appreciable amounts exclusively in C57L mice. Also, altered histology with increased gallbladder wall fibrosis could have contributed to the impairment of gallbladder motility. Impaired gallbladder motility in C57L occurred at an early stage (after 7 days of the lithogenic diet, before gallstones had formed). Therefore, impaired motility could contribute to gallstone formation, even if it would be secondary to hydrophobic bile salts or absorbed cholesterol. The occurrence of su-

persaturated bile (and possibly also hydrophobic bile salt composition) could relate to certain *Lith* genes. A significant number of hepatic lipid regulatory genes, hepatic lipoprotein receptors and related genes, hepatic and intestinal membrane and intracellular lipid transporters, and hepatic lipid regulatory transcription factors that could be involved in the occurrence of biliary cholesterol supersaturation colocalize with various *Lith* genes that were identified by quantitative trait locus studies in the mouse model (for an overview, see 39). In addition, the CCK-A receptor controls to a large extent murine gallbladder contractility, the encoding gene *Cckar* colocalizes with a *Lith* gene on mouse chromosome (39), and targeted disruption of the murine CCK receptor increases susceptibility to gallstones (40). Therefore, *Lith* genes could be involved in the marked differences in gallbladder motility between C57L and AKR mice found in this study.

As inferred from gallbladder-to-hepatic ratios of lipid concentrations, we found a strong decrease of gallbladder absorptive function after institution of the lithogenic diet, particularly in C57L inbred mice. We hypothesize that decreased gallbladder concentrating function could also be secondary to the absorption of cholesterol by the gallbladder wall from supersaturated bile and altered histology with increased gallbladder wall thickness. Our findings of water channel AQP1 expression in apical and basolateral epithelial cell membranes, particularly in the gallbladder neck, are in agreement with previous data (7, 8, 10, 12). The presence of AQP1 in murine gallbladder microvessels (9, 10, 12) has also been reported previously. Recently, AQP8 was detected in the apical gallbladder epithelial plasma membrane of various species, both at the mRNA and protein levels (12). Reduction of AQP expression in the gallbladder epithelial plasma membrane may not be the consequence of a local effect exerted by the lithogenic diet, because concomitant AQP expression in gallbladder endothelial cells appeared not to change. Also, similar AQP8 downregulation was reported recently in the liver of cholesterol-fed mice (41) and during extrahepatic cholestasis (42). We also found, in the current study, significant downregulation of relative AQP1 mRNA expression (from 1 ± 0.12 to 0.48 ± 0.09) and relative AQP8 mRNA expression (from 1 ± 0.08 to 0.57 ± 0.1) in livers of C57L mice after 1 week on the lithogenic diet (results not shown). These findings all suggest that the lithogenic diet exerts a more general effect on AQP expression, possibly because of its high fat and cholesterol contents. With regard to the gallbladder, concordant changes of AQP expression and the absorptive function of this organ on the lithogenic diet, as found in this study, suggest the involvement of these water channels in gallbladder water transport, possibly secondary to changes in electrolyte transport. Gallbladder Na^+ absorption in the fasting state is mostly mediated through apically restricted Na^+/H^+ exchange. This protein kinase C-α-regulated membrane protein facilitates the electroneutral exchange of extracellular Na^+ for intracellular H^+, with subsequent basolateral Na^+ extrusion and secondary osmosis-driven water transport (43). Limited data in the prairie dog model suggest dysfunctional regulation of Na^+/H^+ exchange by protein kinase C-α during gallstone formation (43, 44). Associated Cl^- transfer probably involves Cl^-/HCO_3^- exchangers and chloride channels. In contrast with the fasting state, gallbladder water secretion seems to predominate after meal ingestion, possibly influenced by gastrointestinal hormones such as secretin and vasoactive intestinal polypeptide (45–47). These hormones act on cystic fibrosis-transmembrane conductance regulator in the epithelial cell (47). Increases of intracellular cAMP levels subsequently inhibit Cl^-/HCO_3^- and Na^+/H^+ exchangers at the apical membrane, with the result that net NaCl entry is inhibited (10). Although one may speculate that AQP1 and AQP8 exhibit different functions in the fasting versus the fed state, this remains to be explored in further studies.

Because the lithogenic diet contains significant amounts of the FXR ligand cholic acid, we tested whether AQP1 and AQP8 downregulation could occur through the FXR signaling pathway. Similar AQP downregulation in $FXR^{-/-}$ and corresponding wild-type mice after 1 week of the lithogenic diet argues against a direct role of FXR in driving the lithogenic diet-induced decreases of AQP1 and AQP8 gene expression in gallbladder or liver. This contention is further supported by the absence of any changes in AQP1 and AQP8 gene expression in wild-type mice treated with a synthetic FXR agonist (A. Moschetta and D. J. Mangelsdorf, unpublished observations). In summary, progressive alterations in gallbladder histology during murine lithogenesis are associated with progressively impaired gallbladder motility, particularly in C57L. A temporal association between decreased gallbladder concentrating function and decreased AQP1 or AQP8 expression suggests the involvement of these water channels in gallbladder water transport.

This study was supported by research grants from the Fondo per gli Investimenti della Ricerca di Base (Grant RBAU01R-ANB), Centro di Eccellenza di Genomica in Campo Biomedico ed Agrario, and Progetto Laboratorio Analisi del Gene Studio di Geni di Interesse Biomedico ed Agroalimentare (to G.C. and M. Svelto), by the Howard Hughes Medical Institute (A.M.), by a grant from the Ellison Medical Foundation (to D.Q-H.W.), and by research Grant DK-54012 (to D.Q-H.W.) from the National Institutes of Health (U.S. Public Health Service). The authors thank Prof. Giuseppa E. Liquori for her skillful contribution to the immunohistochemical studies. The authors also thank Dr. Frank Gonzalez for supplying the $FXR^{-/-}$ mice used in this study, Dr. David Mangelsdorf for allowing the $FXR^{-/-}$ mouse experiments to be performed in his laboratory, and Angie Bookout for contributing to the studies in the $FXR^{-/-}$ mouse. The authors are greatly indebted to Helen H-F. Wang (Beth Israel Deaconess Medical Center, Boston, MA) for excellent technical assistance.

REFERENCES

1. Wang, D. Q. H., B. Paigen, and M. C. Carey. 1997. Phenotypic characterization of *Lith* genes that determine susceptibility to

cholesterol cholelithiasis in inbred mice: physical-chemistry of gallbladder bile. *J. Lipid Res.* **38:** 1395–1411.
2. van Erpecum, K. J., D. Q-H. Wang, F. Lammert, B. Paigen, A. K. Groen, and M. C. Carey. 2001. Phenotypic characterization of *Lith* genes that determine susceptibility to cholesterol cholelithiasis in inbred mice: soluble pronucleating proteins in gallbladder and hepatic biles. *J. Hepatol.* **35:** 444–451.
3. van Erpecum, K. J., G. P. vanBerge-Henegouwen, M. F. J. Stolk, W. P. M. Hopman, J. B. M. J. Jansen, and C. B. H. W. Lamers. 1992. Fasting gallbladder volume, postprandial emptying and cholecystokinin release in gallstone patients and normal subjects. *J. Hepatol.* **14:** 194–202.
4. Fridhandler, T. M., J. S. Davison, and E. A. Shaffer. 1983. Defective gallbladder contractility in the ground squirrel and prairie dog during the early stages of cholesterol gallstone formation. *Gastroenterology.* **85:** 830–836.
5. van Erpecum, K. J., G. P. vanBerge-Henegouwen, B. Stoelwinder, Y. M. G. Schmidt, and F. L. H. Willekens. 1990. Bile concentration is a key factor for nucleation of cholesterol crystals and cholesterol saturation index in gallbladder bile of gallstone patients. *Hepatology.* **11:** 1–6.
6. Halpern, Z., M. A. Dudley, M. P. Lynn, J. M. Nader, A. C. Breuer, and R. T. Holzbach. 1986. Vesicle aggregation in model systems of supersaturated bile: relation to crystal nucleation and lipid composition of the vesicular phase. *J. Lipid Res.* **27:** 295–306.
7. Nielsen, S., B. L. Smith, E. I. Christensen, and P. Agre. 1993. Distribution of the aquaporin CHIP in secretory and resorptive epithelia and capillary endothelia. *Proc. Natl. Acad. Sci. USA.* **90:** 7275–7279.
8. Hasegawa, H., S. C. Lian, W. E. Finkbeiner, and A. S. Verkman. 1994. Extrarenal tissue distribution of CHIP28 water channels by in situ hybridization and antibody staining. *Am. J. Physiol.* **266:** C893–C903.
9. Ma, T., S. Jayaraman, K. S. Wang, Y. Song, B. Yang, J. Li, J. A. Bastidas, and A. S. Verkman. 2001. Defective dietary fat processing in transgenic mice lacking aquaporin-1 water channels. *Am. J. Physiol.* **280:** C126–C134.
10. Masyuk, A. I., R. A. Marinelli, and N. F. LaRusso. 2002. Water transport by epithelia of the digestive tract. *Gastroenterology.* **122:** 545–562.
11. Portincasa, P., A. Moschetta, A. Mazzone, G. Palasciano, M. Svelto, and G. Calamita. 2003. Water handling and aquaporins in bile formation: recent advances and research trends. *J. Hepatol.* **39:** 864–874.
12. Calamita, G., D. Ferri, C. Bazzini, A. Mazzone, G. Botta, G. E. Liquori, M. Paulmichl, P. Portincasa, G. Meyer, and M. Svelto. 2005. Expression and subcellular localization of the AQP8 and AQP1 water channels in the mouse gallbladder epithelium. *Biol. Cell.* **97:** 415–423.
13. Lu, T. T., J. J. Repa, and D. J. Mangelsdorf. 2001. Orphan nuclear receptors as eLiXiRs and FiXeRs of sterol metabolism. *J. Biol. Chem.* **276:** 37735–37738.
14. Moschetta, A., A. L. Bookout, and D. J. Mangelsdorf. 2004. Prevention of cholesterol gallstone disease by FXR agonists in a mouse model. *Nat. Med.* **10:** 1352–1358.
15. Makishima, M., A. Y. Okamoto, J. J. Repa, H. Tu, R. M. Learned, A. Luk, M. V. Hull, K. D. Lustig, D. J. Mangelsdorf, and B. Shan. 1999. Identification of a nuclear receptor for bile acids. *Science.* **284:** 1362–1365.
16. Nishina, P. M., J. Verstuyft, and B. Paigen. 1990. Synthetic low and high fat diets for the study of atherosclerosis in the mouse. *J. Lipid Res.* **31:** 859–869.
17. Lammert, F., D. Q. H. Wang, B. Paigen, and M. C. Carey. 1999. Phenotypic characterization of *Lith* genes that determine susceptibility to cholesterol cholelithiasis in inbred mice: integrated activities of hepatic lipid regulatory enzymes. *J. Lipid Res.* **40:** 2080–2090.
18. Wang, D. Q. H., F. Lammert, B. Paigen, and M. C. Carey. 1999. Phenotypic characterization of *Lith* genes that determine susceptibility to cholesterol cholelithiasis in inbred mice: pathophysiology of biliary lipid secretion. *J. Lipid Res.* **40:** 2066–2079.
19. Wang, H. H., N. H. Afdhal, and D. Q. H. Wang. 2004. Estrogen receptor alpha, but not beta, plays a major role in 17beta-estradiol-induced murine cholesterol gallstones. *Gastroenterology.* **127:** 239–249.
20. Wang, D. Q. H. 2002. Aging per se is an independent risk factor for cholesterol gallstone formation in gallstone susceptible mice. *J. Lipid Res.* **43:** 1950–1959.
21. Sinal, C. J., M. Tohkin, M. Miyata, J. M. Ward, G. Lambert, and F. J. Gonzalez. 2000. Targeted disruption of the nuclear receptor FXR/BAR impairs bile acid and lipid homeostasis. *Cell.* **102:** 731–744.
22. Bligh, E. G., and W. J. Dyer. 1959. A rapid method of total lipid extraction and purification. *Can. J Biochem. Physiol.* **37:** 911–917.
23. Fromm, H., P. Hamin, H. Klein, and I. Kupke. 1980. Use of a simple enzymatic assay for cholesterol analysis in human bile. *J. Lipid Res.* **21:** 259–261.
24. Allain, C. C., L. S. Poon, C. S. G. Chan, W. Richmond, and P. C. Fu. 1974. Enzymatic determination of total phospholipids in bile. *J. Clin. Chem.* **20:** 470–475.
25. Turley, S. D., and J. M. Dietschy. 1978. Re-evaluation of the 3 alpha-hydroxysteroid dehydrogenase assay for total bile acids in bile. *J. Lipid Res.* **19:** 924–928.
26. Carey, M. C. 1978. Critical tables for calculating the cholesterol saturation of native bile. *J. Lipid Res.* **19:** 945–955.
27. Rossi, S. S., J. L. Converse, and A. F. Hofmann. 1987. High pressure liquid chromatographic analysis of conjugated bile acids in human bile: simultaneous resolution of sulfated and unsulfated lithocholyl amidates and the common conjugated bile acids. *J. Lipid Res.* **28:** 589–595.
28. Ferri, D., A. Mazzone, G. E. Liquori, G. Cassano, M. Svelto, and G. Calamita. 2003. Ontogeny, distribution, and possible functional implications of an unusual aquaporin, AQP8, in mouse liver. *Hepatology.* **38:** 947–957.
29. Graham, R. C., Jr., and M. J. Karnovsky. 1966. The early stages of absorption of injected horseradish peroxidase in the proximal tubules of mouse kidney: ultrastructural cytochemistry by a new technique. *J. Histochem. Cytochem.* **14:** 291–302.
30. Bookout, A. L., and D. J. Mangelsdorf. 2003. A quantitative real-time PCR protocol for analysis of nuclear receptor pathways. *NURSA e-Journal.* Vol. 1 doi: 10.1621/nrs.01012.
31. Corradini, S. G., C. Ripani, P. Della Guardia, L. Giovannelli, W. Elisei, A. Cantafora, M. C. Pisanelli, G. D. Tebala, G. Nuzzo, A. Corsi, et al. 1998. The human gallbladder increases cholesterol solubility in bile by differential lipid absorption: a study using a new in vitro model of isolated intra-arterially perfused gallbladder. *Hepatology.* **28:** 314–322.
32. Behar, J., K. Y. Lee, W. R. Thompson, and P. Biancani. 1989. Gallbladder contraction in patients with pigment and cholesterol stones. *Gastroenterology.* **97:** 1479–1484.
33. Gallinger, S., P. R. C. Harvey, C. N. Petrunka, R. G. Ilson, and S. M. Strasberg. 1987. Biliary proteins and the nucleation defect in cholesterol cholelithiasis. *Gastroenterology.* **92:** 867–875.
34. Carey, M. C., and D. M. Small. 1978. The physical chemistry of cholesterol solubility in bile. Relation to gallstone formation and dissolution in man. *J. Clin. Invest.* **61:** 998–1026.
35. Tauscher, A., and R. Kuver. 2003. ABCG5 and ABCG8 are expressed in gallbladder epithelial cells. *Biochem. Biophys. Res. Commun.* **307:** 1021–1028.
36. Miquel, J. F., M. Moreno, L. Amigo, H. Molina, P. Mardones, I. I. Wistuba, and A. Rigotti. 2003. Expression and regulation of scavenger receptor class B type I (SR-BI) in gall bladder epithelium. *Gut.* **52:** 1017–1024.
37. Erranz, B., J. F. Miquel, W. S. Argraves, J. L. Barth, F. Pimentel, and M. P. Marzolo. 2004. Megalin and cubilin expression in gallbladder epithelium and regulation by bile acids. *J. Lipid Res.* **45:** 2185–2198.
38. Xu, Q. W., S. M. Freedman, and E. A. Shaffer. 1997. Inhibitory effect of bile salts on gallbladder smooth muscle contractility in the guinea pig in vitro. *Gastroenterology.* **112:** 1699–1706.
39. Lammert, F., M. C. Carey, and B. Paigen. 2001. Chromosomal organization of candidate genes involved in cholesterol gallstone formation: a murine gallstone map. *Gastroenterology.* **120:** 221–238.
40. Wang, D. Q., F. Schmitz, A. S. Kopin, and M. C. Carey. 2004. Targeted disruption of the murine cholecystokinin-1 receptor promotes intestinal cholesterol absorption and susceptibility to cholesterol cholelithiasis. *J. Clin. Invest.* **114:** 521–528.
41. Maxwell, K. N., R. E. Soccio, E. M. Duncan, E. Schayek, and J. L. Breslow. 2003. Novel putative SREBP and LXR target genes identified by microarray analysis in liver of cholesterol-fed mice. *J. Lipid Res.* **44:** 2109–2119.

42. Carreras, F. I., S. A. Gradilone, A. Mazzone, F. Garcia, B. Q. Huang, J. E. Ochoa, P. S. Tietz, N. F. LaRusso, G. Calamita, and R. A. Marinelli. 2003. Rat hepatocyte aquaporin-8 water channels are down-regulated in extrahepatic cholestasis. *Hepatology.* **37:** 1026–1033.
43. Narins, S. C., R. Ramakrishnan, E. H. Park, P. B. Bolno, D. A. Haggerty, P. R. Smith, W. C. Meyers, and M. Z. Abedin. 2005. Protein kinase C-alpha regulation of gallbladder Na^+ transport becomes progressively more dysfunctional during gallstone formation. *J. Lab. Clin. Med.* **146:** 227–237.
44. van Erpecum, K. J., and D. Q. H. Wang. 2005. The gallbladder: innocent bystander or major factor in cholesterol-gallstone formation? *J. Lab. Clin. Med.* **146:** 202–204.
45. Igimi, H., F. Yamamoto, and S. P. Lee. 1992. Gallbladder mucosal function: studies in absorption and secretion in humans and in dog gallbladder epithelium. *Am. J. Physiol.* **263:** G69–G74.
46. Sweeting, J. G. 1993. Does the gallbladder secrete? *Gastroenterology.* **104:** 329–330.
47. Peters, R. H., J. H. van Doorninck, P. J. French, R. Ratcliff, M. J. Evans, W. H. Colledge, J. Bijman, and B. J. Scholte. 1997. Cystic fibrosis transmembrane conductance regulator mediates the cyclic adenosine monophosphate-induced fluid secretion but not the inhibition of resorption in mouse gallbladder epithelium. *Hepatology.* **25:** 270–277.
48. Whitlock, R. T., and H. O. Wheeler. 1964. Coupled transport of solute and water across rabbit gallbladder epithelium. *J. Clin. Invest.* **43:** 2249–2265.